

EFFICIENT IMAGE RESTORATION USING CELLULAR NEURAL NETWORKS

Mehmet E. Çelebi

*Cüneyt Güzelis**

Faculty of Electrical-Electronics Engineering
İstanbul Technical Univ., İstanbul, Maslak 80626, Turkey
celebi@ehb.itu.edu.tr guzelis@ehb.itu.edu.tr

ABSTRACT

In this paper, a 3-D Cellular Neural Network (CNN) is applied for restoration of degraded images. It is known that regularized or Maximum a Posteriori estimation based image restoration problems can be formulated as the minimization of the Lyapunov function of the discrete-time Hopfield network. Recently, this Lyapunov function based design method has been extended to the continuous-time Hopfield network and to the continuous-time CNN operating either in a binary steady-state output mode or in a real-valued steady-state output mode. This paper considers 3-D CNN in the binary mode, which needs eight binary (nonredundant) neurons only for each image pixel thus reducing the computational overhead, and introduces a hardware annealing approach to overcome bad local minima problem due to binary mode of operation and nonredundant representation.

1. INTRODUCTION

Image restoration refers to the problem of estimating the ideal image from its blurred and noisy rendition. Recently, there is a surge of interest to solve image restoration problems using neural networks [1]-[6].

The earliest attempt, in this regard, was by Zhou et.al. [1] where equivalencies between the image restoration cost function and the Lyapunov function of the discrete-time Hopfield network are investigated. However, their network has negative self feedback connection weights, thus, they introduced an energy function check-up step which is ad hoc, time consuming solution. To overcome negative self-feedback problem, Paik and Katsagellos [2] suggested several modifications of the discrete Hopfield network. Figueiredo and Leitao [3] investigated neural implementations of iterative restoration schemes.

More recently, there have been attempts [4]-[6] to include CNNs [7] for image restoration problems. Unal [4] devised an algorithm which splits bit images and treats every bit image separately. The interrelations among bit images are omitted, however. In another attempt, Miller et.al. [5] formulated the image restoration problem as solving linear equations by means of differential equations, and imbedded those equations into the dynamics of CNN with linear

output function. In [6], both continuous-time Hopfield Network and continuous-time CNN operating either in a binary mode of steady-state output or in a real-valued mode of steady-state output were introduced for restoration of noisy and blurry images, and a comparison was made over the existing neural network algorithms. Among those networks considered, the 3-D CNN operating in the binary mode needs only eight neurons to represent 256 gray levels for each pixel. However, since nonredundant (eight-bit) neurons were used, undesirable local minimum solutions were obtained precluding the efficiency of the algorithms under consideration. If redundant neurons, namely, 256 neurons were used to represent each pixel gray level as had been done in [1]-[3], one may argue that better solutions may have been obtained, since, for such a case there are redundantly many global optimal solutions, and, thus there is a greater chance to end up with one of them. Indeed, no problem concerning the quality of the solutions had been reported [1]-[3]. This simple sum representation [8] has obviously a quite of computational burden. It is therefore better to insist on nonredundant representation and try to improve the quality of the solutions obtained through nonredundant representation. In this paper, we therefore propose a hardware annealing method [10]-[11] associated with a graduated nonconvexity approach to cope with the bad local minimum problem.

This paper is organized as follows: In Section 2, the 3-D CNN model considered in this paper is briefly described. In Section 3, we formulate our graduated nonconvexity type algorithm which ameliorates the quality of final solutions. In Section 4, experimental results are given to support our reasoning. Finally, in Section 5, we draw our final conclusions.

2. CELLULAR NEURAL NETWORKS

A 3-D continuous-time CNN which was originally developed as a 2-D array of first-order dynamical cells [1] and then generalized to the n-D, multi-layer, higher-order case [9] is described in (1). The cells in a CNN are connected only to the cells in their nearest neighborhood of size r , i.e., $N_r(\mathbf{i})$, defined as : $N_r(\mathbf{i}) = \{ \hat{\mathbf{i}} \mid D(\mathbf{i}; \hat{\mathbf{i}}) \leq r \}$. Where, $\mathbf{i} = (i_1, i_2, i_3)$ is the vector of integers indexing the cell $C(\mathbf{i})$, r is the neighborhood size ; and $D(\mathbf{i}; \hat{\mathbf{i}})$ denotes the

*This work was supported in part by Turkish State Planning Office, Turkish Scientific Research Council and İstanbul Technical University.

metric $D(\hat{\mathbf{i}}; \hat{\mathbf{i}}) = \max\{|i_1 - \hat{i}_1|, |i_2 - \hat{i}_2|, |i_3 - \hat{i}_3|\}$.

$$\begin{aligned} \dot{x}_i &= -A \cdot x_i + \sum_{\hat{\mathbf{i}} \in N_r(i)} w_{i,\hat{\mathbf{i}}} \cdot y_{\hat{\mathbf{i}}} + \sum_{\hat{\mathbf{i}} \in N_r(i)} z_{i,\hat{\mathbf{i}}} \cdot u_{\hat{\mathbf{i}}} + I. \\ y_i &= f(x_i) \stackrel{\text{def}}{=} \frac{1}{2} \cdot \{|x_i + 1| - |x_i - 1|\}. \end{aligned} \quad (1)$$

Where, $A, I, w_{i,\hat{\mathbf{i}}}$ and $z_{i,\hat{\mathbf{i}}} \in \mathbf{R}$ are constants. u_i, x_i , and y_i denotes the input, the state, and the output of the cell $C(\mathbf{i})$, respectively. $|\cdot|$ denotes the absolute value function.

It is shown in [7] that if the feedback connection weights $w_{i,\hat{\mathbf{i}}}$ are symmetric, then CNN is completely stable, i.e., each trajectory tends, as time goes to infinity, to one of the equilibria. In this paper the input connection weights $z_{i,\hat{\mathbf{i}}}$ are chosen symmetric for reducing computational costs and so are the feedback connection weights $w_{i,\hat{\mathbf{i}}}$ for ensuring the complete stability. The feedback and input template coefficients satisfy the space-invariant property, i.e., $w_{i,\hat{\mathbf{i}}} = W_{i-\hat{\mathbf{i}}}$, $z_{i,\hat{\mathbf{i}}} = Z_{i-\hat{\mathbf{i}}}$.

The completely stable CNNs can operate either in the bipolar binary steady-state output mode or in the real-valued steady-state output mode. The first mode which is considered in this paper can be ensured [7] by the constraint $w_{i,i} > A$. If this constraint is not satisfied, then the steady-state outputs of the cells may take real values now allowing to process gray-level data by just one 2-D CNN layer. The latter mode of operation is used in [5]-[6].

The Lyapunov function for a CNN layer proposed in [7] for proving the complete stability under the symmetric connection weights assumption is given in Equation (2):

$$\begin{aligned} E_{CNN} \stackrel{\text{def}}{=} & -\frac{1}{2} \sum_i \sum_{\hat{\mathbf{i}} \in N_r(i)} w_{i,\hat{\mathbf{i}}} \cdot y_i \cdot y_{\hat{\mathbf{i}}} + \frac{A}{2} \sum_i y_i^2 \\ & - \sum_i \sum_{\hat{\mathbf{i}} \in N_r(i)} z_{i,\hat{\mathbf{i}}} \cdot y_i \cdot u_{\hat{\mathbf{i}}} - \sum_i I \cdot y_i. \end{aligned} \quad (2)$$

3. A HARDWARE ANNEALING SOLUTION TO THE IMAGE RESTORATION PROBLEM

Using continuous-time CNN for image restoration has some advantages over discrete-time or continuous-time Hopfield networks. First, CNN have purely quadratic Lyapunov function which occurs in image restoration. Second, their self-feedback coefficients need not be zero (or negative) which is a requirement for discrete-time Hopfield network. CNN always converges to a local minimum solution as long as the symmetry condition is satisfied. Finally, because of parallel and fast operation, continuous-time neural networks are best candidates for real-time optimization problems [10]-[11].

In most of the image restoration schemes, the degradation model is given by the following 2-D FIR blurring system with the additive noise.

$$d_{i_1,i_2} = \sum_{(\hat{i}_1,\hat{i}_2) \in N_r(0,0)} h_{i_1,\hat{i}_2} \cdot \hat{y}_{i_1-\hat{i}_1,i_2-\hat{i}_2} + n_{i_1,i_2}.$$

Where, h_{i_1,i_2} is the 2-D impulse response of the FIR blurring system commonly known as point spread function. \hat{y}_{i_1,i_2} , d_{i_1,i_2} , and n_{i_1,i_2} represents the intensity gray levels of the original image, the observation, and the white Gaussian noise process, respectively.

In both regularization and Maximum a Posteriori estimation frameworks, the image restoration for the above degradation model can be posed as the minimization of the following cost function.

$$\begin{aligned} \Psi \stackrel{\text{def}}{=} & \frac{1}{2} \cdot \sum_{(i_1,i_2)} \left(d_{i_1,i_2} - \sum_{(\hat{i}_1,\hat{i}_2) \in N_r(0,0)} h_{i_1,\hat{i}_2} \cdot y_{i_1-\hat{i}_1,i_2-\hat{i}_2} \right)^2 \\ & + \frac{\lambda}{2} \cdot \sum_{(i_1,i_2)} \left(\sum_{(\hat{i}_1,\hat{i}_2) \in N_r(0,0)} g_{i_1,\hat{i}_2} \cdot y_{i_1-\hat{i}_1,i_2-\hat{i}_2} \right)^2. \end{aligned} \quad (3)$$

Where y_{i_1,i_2} 's represent an estimate of the original image. λ represents the regularization parameter and g_{i_1,i_2} is the impulse response of an FIR high pass filter which is an approximation to the Laplacian operator.

It should be observed that the cost function in (3) and the Lyapunov function in (2) have similar quadratic forms and they can be made equivalent by choosing suitable connection weights.

In order to handle gray-level images with CNNs operating in the bipolar binary steady-state output mode, eight cells are needed for each image pixel if the binary representation is used. 3-D CNN such that the third dimension is for the gray-levels can be used for this purpose. In the binary representation, each pixel gray-level y_{i_1,i_2} , in the range of $[-127.5, 127.5]$, can be given in terms of the bipolar binary outputs $y_{i_1,i_2,i_3} \in \{-1, 1\}$ as

$$y_{i_1,i_2} = \sum_{i_3=0}^7 y_{i_1,i_2,i_3} \cdot 2^{i_3-1}.$$

If the binary sum representation is used also for the pixel gray-levels d_{i_1,i_2} of the observed image, then Ψ_{Binary} which is obtained from Ψ by adding a new term forcing y_{i_1,i_2,i_3} 's

to take binary values, and it can be made equivalent to the Lyapunov function in (2) for the 3-D CNN.

$$\Psi_{Binary} = \Psi - \frac{1}{2} \cdot \sum_{(i_1, i_2, i_3)} \alpha_{i_1, i_2} \cdot 2^{i_3-1} \cdot (y_{i_1, i_2, i_3})^2 . \quad (4)$$

The Lyapunov function in (2) for a 3-D continuous-time CNN becomes equivalent to the cost function in (3) if

I) the following constant term which has no effect on the minimization is ignored

$$\frac{1}{2} \cdot \sum_{(i_1, i_2)} (d_{i_1, i_2})^2 ,$$

II) the external input is chosen equal to the observed image, i.e., $u_{i_1, i_2} = d_{i_1, i_2}$,

III) the threshold I is set to zero,

IV) $z_{i_1, i_2, i_3; \hat{i}_1, \hat{i}_2, \hat{i}_3} = h_{i_1 - \hat{i}_1, i_2 - \hat{i}_2} \cdot 2^{i_3 + \hat{i}_3 - 2}$,

V) for all $i_1 \neq \hat{i}_1, i_2 \neq \hat{i}_2, i_3 \neq \hat{i}_3$,

$$\begin{aligned} w_{i_1, i_2, i_3; \hat{i}_1, \hat{i}_2, \hat{i}_3} = & \\ & - \sum_{\bar{i}_1, \bar{i}_2 \in N_r(0,0)} h_{\bar{i}_1, \bar{i}_2} \cdot h_{\bar{i}_1 + \hat{i}_1 - i_1, \bar{i}_2 + \hat{i}_2 - i_2} \cdot 2^{i_3 + \hat{i}_3 - 2} \\ & + \lambda \cdot \sum_{\bar{i}_1, \bar{i}_2 \in N_r(0,0)} g_{\bar{i}_1, \bar{i}_2} \cdot g_{\bar{i}_1 + \hat{i}_1 - i_1, \bar{i}_2 + \hat{i}_2 - i_2} \cdot 2^{i_3 + \hat{i}_3 - 2} , \quad (5) \end{aligned}$$

VI) for all i_1, i_2, i_3 ,

$$\begin{aligned} w_{i_1, i_2, i_3; i_1, i_2, i_3} = & \\ & A - \sum_{\bar{i}_1, \bar{i}_2 \in N_r(0,0)} (h_{\bar{i}_1, \bar{i}_2})^2 \cdot 2^{2 \cdot i_3 - 2} \\ & - \lambda \cdot \sum_{\bar{i}_1, \bar{i}_2 \in N_r(0,0)} (g_{\bar{i}_1, \bar{i}_2})^2 \cdot 2^{2 \cdot i_3 - 2} + \alpha_{i_1, i_2} \cdot 2^{2 \cdot i_3 - 2} . \quad (6) \end{aligned}$$

It should be observed that the self-feedback connection weights in VI) can be made greater than A by choosing sufficiently large α_{i_1, i_2} values, and then the bipolar binary

steady-state output mode for the 3-D CNN can be ensured. Note also that adding squared terms as in (4) does not affect the outcome of the optimization. In this work, we choose the parameter α_{i_1, i_2} space-invariant, namely, $\alpha_{i_1, i_2} = \alpha$. In [6], a fixed α was chosen yielding undesirable local minimum solutions. Therefore an effective way to improve the quality of the final solutions is needed.

Hardware annealing is an efficient electronic version of the mean field annealing, and has been successfully used in the past to find the global optimum solutions of some optimization problems [11]. On the other hand, graduated nonconvexity method is employed to solve nonconvex optimization problems by first transforming the cost function into a convex one, and then gradually rendering it nonconvex [10]. It is therefore desired to unite the properties of both algorithms to overcome undesirable local minimum problem. Now, considering the quadratic cost function in (4) we can make several observations: i) For $\alpha < 0$ the quadratic in (4) is convex. ii) For $\alpha > 0$ the quadratic in (4) is indefinite and may even become concave for increasing α . iii) For $\alpha > 1$ the binary mode of operation is ensured. We therefore describe our algorithm as follows: First allow α to be slightly negative so that the output is close to the unconstrained minima of the convex cost function. Later slowly increase α to be slightly greater than unity for binary mode of output.

4. EXPERIMENTAL RESULTS

In order to test the validity of the results developed in the previous sections, two experiments are performed upon the 64x64 mid-portion of the original ‘‘Lena’’ image seen in Figure (a), and its degraded version seen in Figure (b). In the experiments, the nonlinear differential equations are simulated using forward Euler method with sufficiently small step size. The blurring system used in the experiments is given by the following delta response.

$$h_{i_1, i_2} = \begin{cases} \frac{1}{5} & i_1 = 0, i_2 = 0 \\ \frac{1}{10} & |i_1|, |i_2| \leq 1, i_1, i_2 \neq 0 \end{cases} .$$

The regularizing function g_{i_1, i_2} is chosen as the discrete Laplacian operator. First experiment is performed with a fixed $\alpha = 1.1$. The outcome of the experiment can be seen in Figure (c). In the second experiment α is time varying (annealed) with $\alpha(t) = 1.1 - 1.2e^{-t/\tau}$ with a suitable time-constant τ . The outcome of that experiment can be seen in Figure (d). As it can be observed, there is a considerable improvement compared to first experiment. With A chosen to be unity, our simulations show that the first experiment lasts about 40 seconds, and the second experiment lasts about 150 seconds. Note that, considering typical circuit dynamics in VLSI implementations, one may have a millionfold reduction of durations.

5. CONCLUSION

In this paper, regularized and MAP image restoration problems have been formulated as the minimization of the Lyapunov functions of a 3-D CNN operating in a binary steady-state output mode which is ensured by adding an extra term

to the image restoration cost function. A hardware annealing approach has been introduced for obtaining better local minimum solutions for the considered image restoration problem. The experiments demonstrate that continuous-time CNN is a very good candidate for real-time image restoration since a possible VLSI implementation of it may take few microseconds to restore an image of any size due to parallel operation.

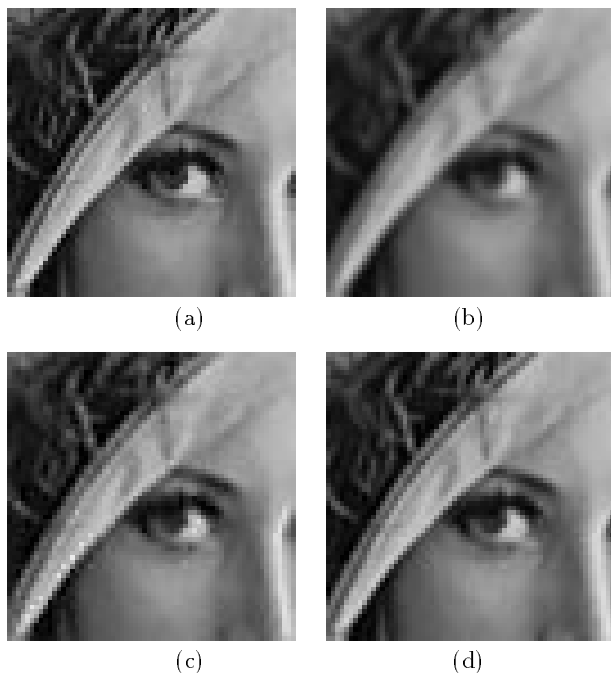


Figure (a) Original "Lena" image. (b) The blurred image ($S/N = 14dB$). (c) The restored image with unannealed CNN ($S/N = 16dB$). (d) The restored image with annealed CNN ($S/N = 21dB$).

REFERENCES

- [1] Y. T. Zhou, R. Chellapa, and B. K. Jenkins, "Image restoration using a neural network," IEEE Trans. Acoust. Speech, Signal Processing, Vol. ASSP-36, pp. 1141-1151, 1988.
- [2] J. K. Paik and A. K. Katsaggelos, "Image restoration using a modified Hopfield network," IEEE Trans. Image Processing, Vol. 1, pp. 49-63, January 1992.
- [3] M. A. T. Figueiredo and J. M. N. Leitao, "Sequential and parallel image restoration: neural network implementations," IEEE Trans. Image Processing, Vol. 3, pp. 789-801, November 1994.
- [4] A. Ünal, Image Restoration Using Dynamical Neural Networks, M.Sc. Thesis, İstanbul Technical University, June 1994.
- [5] J. P. Miller, T. Roska, T. Sziranyi, K. R. Crouse, L. O. Chua, and L. Nemes, "Deblurring of images by cellular neural networks with applications to microscopy," IEEE Int. Workshop on Cellular Neural Networks and their Applications, Rome, December 18-21 1994.
- [6] M. E. Çelebi and C. Güzeliş, "Lyapunov Function Based Design of Dynamical Neural Networks for Restoration of Blurry and Noisy Images," IEEE Int. Conf. on Neural Networks (ICNN), Perth, pp. 1913-18, 1995.
- [7] L. O. Chua, and L. Yang, "Cellular neural networks: Theory and Applications," IEEE Trans. Circuits Syst. Vol. 35, No. 10, pp. 1257-1272, October 1988.
- [8] M. Takeda and J. W. Goodman, "Neural networks for computation: number representations and programming complexity," Applied Optics, Vol. 25, No. 18, September 1986.
- [9] C. Güzeliş and L. O. Chua, "Stability analysis of generalized cellular neural networks," Int. J. Circuit Theory and Appl., Vol. 21, pp. 1-33, January-February 1993.
- [10] A. Cichocki and R. Unbehauen, "Neural networks for optimization and signal processing," John Wiley Sons, 1993.
- [11] S. H. Bang, B. J. Sheu and E. Y. Chou, "A hardware annealing method for optimal solutions on cellular neural networks," IEEE Trans. Circuits Syst., Part-II, Vol. 43, No. 6, pp. 409-421, June 1996.